

REMOVAL OF PHOSPHATE SPECIES FROM WASTEWATER USING AUTOCLAVED CELLULAR CONCRETE AND PUMICE STONE

Oanamari Daniela ORBULEȚ¹, Gabriel GÂRLEANU^{2*}, Mirela CIŞMAŞU (ENACHE)¹, Elena Raluca CÂRJILĂ (MIHALACHE)¹, Adina-Alexandra SCARLAT (MATEI)¹, Denisa Nicoleta AIRINEI¹, Adriana Ionela MIU (MIHAIL)¹, Mădălina GRINZEANU¹, Cristina MODROGAN¹

Phosphates are key pollutants contributing to water eutrophication. This study investigated phosphate removal from wastewater using cost-effective adsorbents: autoclaved cellular concrete (ACC) and pumice stone (PS). Adsorption experiments at pH 3 and 9 were analyzed with Langmuir and Freundlich isotherms, and kinetic data were evaluated using pseudo-second-order and Langmuir-Hinshelwood models. Results showed adsorption efficiency depends critically on pH, with Freundlich isotherm ($R^2 = 0.90 \div 0.97$) better describing the heterogeneous adsorbent surfaces compared to Langmuir ($R^2 = 0.82 \div 0.92$). Kinetics aligned with the pseudo-second-order model. Both materials proved effective for phosphate removal, offering practical solutions for wastewater treatment.

Keywords: Phosphate adsorption; Wastewater; Sorption capacity; Pumice stone; Autoclaved cellular concrete

1. Introduction

The presence of large amounts of phosphate ions in the water resources has become a major concern, especially in the context of global climate change which accentuates the decay of water quality and the water scarcity. Low amounts of phosphate ions are needed for the development of living organisms in water environments. However, water resources are threatened by the discharge of waste waters (industrial or urban) with an important load of phosphate ions, waters coming especially from wastewater treatment plants, infiltration through the excessive use of fertilizers, the discharge of industrial waters and deposition from the atmosphere. This results in an excess of phosphate ions that cannot be assimilated by the living organisms from the receiving waters. An increase of the bioavailability of phosphate ions will enhance the algae development [1]. Without any measure taken, the algae blooming will eventually lead to the process of water eutrophication [2]. The eutrophication decreases the water quality as a source of

¹ Faculty of Chemical Engineering and Biotechnologies, National University of Science and Technology POLITEHNICA Bucharest, Romania

² Department of Quality Engineering and Industrial Technologies, National University of Science and Technology POLITEHNICA Bucharest, Romania, corresponding author, e-mail: gabriel.garleanu@upb.ro

drinking water. The cost of water potabilization is significantly increased because of supplementary steps introduced by using a low-quality water source [3].

In the last years, because of the decreasing of availability of water resources, new legislation with stricter maximum allowed levels of phosphate in effluents was introduced. According to the European legislation, three directions must be followed (i) a good management of fertilizer used for soils amendment, (ii) reducing the levels of P in wastewater and (iii) implement the phosphate ions recovery and reuse [4]. Phosphate ions recovery from wastewater allows them to sustainably provide mineral resources of phosphate ions and avoid water eutrophication. The limit values of phosphorus in discharged effluents as given in the laws adopted by the European Parliament are given in Table 1.

Table 1

Limit values (according to European directives) of phosphorus loading in municipal and industrial wastewater.

Quality indicator	M.U.	Limit values	Reference
Total phosphorus	mg/L	<p style="text-align: center;">1 for regions with p.e. (population equivalent) between 10 000 and 100 000</p> <p style="text-align: center;">2 for regions with p.e. higher than 100 000</p>	Council Directive 91/271/EEC of 21 May 1991 concerning urban waste-water treatment [5, 6]

Note: European regulations often refer to the concentration of total phosphorus (P) in mg/L, rather than indicating the concentration of phosphate ions directly. To convert these values into terms of phosphate ions (PO_4^{3-}), the ratio of molar masses is used: which means that $1 \text{ mg/L P} \approx 3.06 \text{ mg/L } \text{PO}_4^{3-}$.

Implementation of the use of P free detergents starting with the year 2000 has contributed to the reducing of the residual P loading in urban wastewater [7]. Work still needs to be done concerning the adequate use of fertilizers and the management of agricultural waste (manure) from farms [8-10].

The methods used to reduce the phosphate content in effluents in wastewater treatment plants are applied to sewage and sludge. These methods include precipitation [11], crystallization [12, 13], adsorption [14], electrochemical methods [15], membrane separation [16] and biological methods [17, 18]. Depending on the phosphate ions concentration in the effluent and the removal method, an initial step of sewage concentration may be needed to make phosphate ions recovery efficient. Among the above-mentioned methods, adsorption is highly efficient, can be applied to a large range of concentrations and depending on the adsorbent material can have a lower cost [19, 20]. The adsorbent materials must be very porous (large specific surface area), have a good adsorption capacity towards phosphate ions, easily available, low cost, non-toxic [21]. The possibility of reuse of the adsorbent with the removed phosphate ions makes adsorption a very good

method to be applied in the context of circular economy applied to phosphate ions [22].

The aim of this work is to evaluate the feasibility of using easily available adsorbents in phosphate removal from waste waters. For that we have tested two materials: pumice stone (PS) and autoclaved cellular concrete (ACC), for phosphate removal from aqueous solutions. The effect of experimental conditions e.g. pH (3 or 9), initial phosphate concentration and the contact time, were presented. The selection of these two pH values allows for the observation of adsorption behavior under typical conditions for: acidic waters, such as those polluted by the mining or chemical industries, and basic waters, such as those resulting from certain industrial processes or improperly treated effluents. By comparing the results at these two pH values, the optimal operating range of the adsorbents can be determined, and recommendations can be made regarding potential pH adjustment steps in practical applications. The results were interpreted using adsorption isotherms (Langmuir and Freundlich) and kinetic models (first order and pseudo second order Langmuir-Hinshelwood models). Depending on the pH, phosphate ions exist in different ionic forms: H_3PO_4 (pH < 2), $H_2PO_4^-$ (pH = 2–7), HPO_4^{2-} (pH = 7–12), and PO_4^{3-} (pH > 12). In the present study, at pH 3, $H_2PO_4^-$ is predominantly removed, while at pH 9, HPO_4^{2-} is targeted. These transformations justify the selection of the two pH values.

Results have shown that both materials have better adsorption capacity of phosphate in acidic conditions (pH = 3).

2. Materials and Methods

2.1. Materials and reagents

2.1.1. Pumice stone material

Pumice is a natural material of volcanic origin [23], successfully used in the adsorption of different pollutants (e.g. nitrate, ammonium, heavy metals, humic acid, dyes etc) from aqueous systems [24-28]. It can be used as an adsorbent or as a support for other materials in adsorption processes [29]. Pumice was purchased from Forster's Natural Products - Made in Germany. The chemical composition of the PS was performed by XRF (X-ray Fluorescence) analysis (using a X-ray fluorescence spectrometer – MiniPal PW4025) and the results are presented in Table 2.

Table 2

Chemical composition of PS

Compound	SiO ₂	Al ₂ O ₃	Fe ₂ O ₃	CaO	MnO	Others
Concentration %	51.26	14.84	3.16	28.08	0.099	2.54

The XRD patterns for initial PS sample and for PS after being kept at pH = 3 are given in Fig. 1 and confirm the crystalline structure of the material presenting sharp peaks. The XRD spectra of initial PS sample shows three main components

($x\text{CaO SiO}_2 z\text{H}_2\text{O}$, SiO_2 and $\text{K}_2\text{Ca}_6\text{Si}_4\text{O}_{15}$). The sample that was kept at $\text{pH} = 3$ (Fig. 1b) in the presence of phosphate ions shows same phase rearrangements and the presence of five components ($x\text{CaO SiO}_2 z\text{H}_2\text{O}$, SiO_2 , Mn_2O_3 , $\text{K}_3(\text{MnH}_4)\text{H}$, $\text{Mg}_2\text{P}_2\text{O}_7$).

According to International Union of Geological Sciences (IUGS), the magmas are classified in fresh and altered. The fresh rocks are classified depending on their character in acidic, intermediate, basic, and ultrabasic, while for the altered ones no classifications criteria are advised [30]. The properties of pumice stone are derived from its composition (the majority component is SiO_2) and its highly porous structure developed during the evacuation of gases through the lava in the cooling process of the lava. They give the material a light weight with a stable mechanical structure [31].

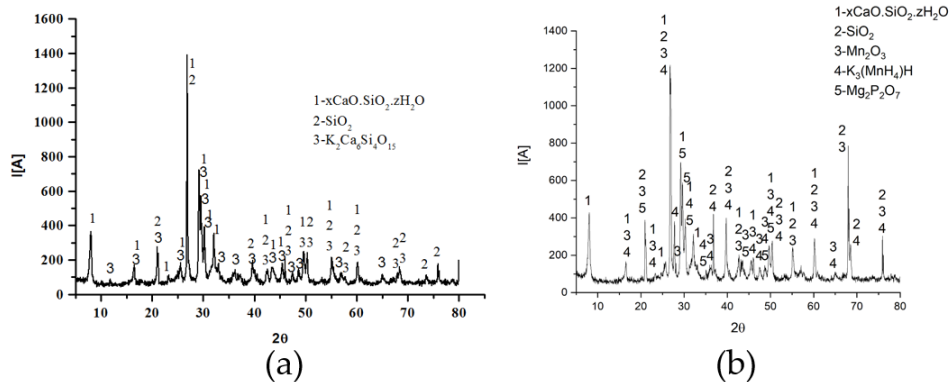


Fig. 1. XRD patterns of PS (a) initial material, (b) at $\text{pH} = 3$

The mechanical and the durability of PS are so good that it has been also included as an additive in the materials used for old building repairs [32]. In addition, it is also a very stable material from a chemical point of view (it does not release secondary pollutants when in contact with water), which makes it a good candidate in adsorption operations. Another advantage is linked with the material availability and its low price. In addition, there are studies that have indicated that pumice stone is an ideal support for metal impregnation on its surface [33-35]. This makes very interesting to study the ability of pumice stone to remove pollutants from wastewater [27, 36-38].

The specific surface was determined by the Brunauer-Emmett-Teller (BET) method. The samples were adsorption-desorption isotherms were obtained at 77 K with an Autosorb⁻¹ Quantachrome Instruments analyzer. The specific surface of initial PS sample used in our experiments is $16.38 \text{ m}^2/\text{g}$ (and the average pore size is 11.3 nm) which slightly higher than previous values reported in the literature [28, 38, 39]. The value of the sample at acidic pH (3) is slightly higher than the initial

sample, $20.96 \text{ m}^2/\text{g}$ (and average pore size 9.3 nm) indicating some pore structure modifications at lower pH.

2.1.2. Autoclaved Cellular Concrete

Autoclaved cellular concrete (ACC) is a construction material, included in the category of lightweight concrete. It is manufactured from various mixtures of sand, cement, lime, water [40, 41]. It has a good mechanical strength and high specific surface area given by the porous structure obtained via gas releases during the manufacturing process [42, 43]. Like the PS, ACC does not release hazardous compounds when it is put in contact with the water [44]. All this and the relatively low price mean that ACC also stands as a good candidate for use in the adsorption of dangerous compounds from wastewaters [45].

The XRD patterns for initial ACC sample and for ACC after being kept at $\text{pH} = 3$ are given in Fig. 2. The sharp peaks in the XRD patterns confirm the crystalline structure of the ACC material. The XRD spectra of initial ACC sample shows four components (Ca_2SiO_4 , SiO_2 , $\text{Mg}_{0.06}\text{Ca}_{0.94}\text{CO}_3$ and Al_2O_3). The sample that was kept at $\text{pH} = 3$ (Fig. 2b) in the presence of phosphate ions shows same phase rearrangements and the presence of five crystalline components (Ca_2SiO_4 , SiO_2 , $\text{Mg}_{0.06}\text{Ca}_{0.94}\text{CO}_3$, $\text{MgHPO}_4 \cdot \text{H}_2\text{O}$ and $\text{Ca}_{0.05}\text{Al}_{0.1}\text{Si}_{1.9}\text{O}_4$).

The chemical composition of the ACC sample as determined by XRF analysis is given in Table 3. Like in the case of PS, the main oxide is SiO_2 , followed by CaO and Al_2O_3 .

Table 3

Chemical composition for ACC

Compound	SiO_2	Al_2O_3	Fe_2O_3	CaO	MnO	Others
Concentration, %	61.01	13.05	2.93	21.73	0.078	1.2

The specific surface of initial ACC sample used in our experiments is $30.99 \text{ m}^2/\text{g}$ and average pore size 9.2 nm which is in agreement with previously reported values [46, 47].

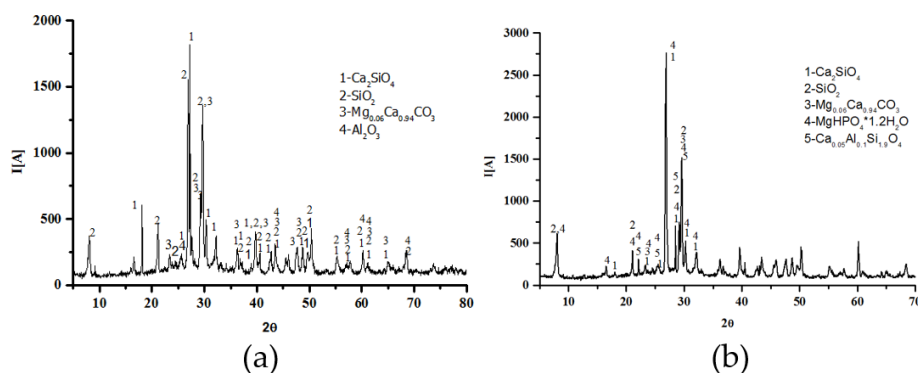


Fig. 2. XRD patterns of ACC (a) initial material, (b) at $\text{pH} = 3$

The value of the sample at acidic pH (3) is slightly lower than the initial sample, $23.86 \text{ m}^2/\text{g}$ and average pore size 9.6 nm indicating a slight reduction of number of pores at lower pH.

2.1.3. Chemical Reagents

KH_2PO_4 were purchased from Sigma Aldrich (Merck KGaA, Darmstadt, Germany). Natrium hidroxid (NaOH) and sulfuric acid (H_2SO_4) were purchased from Sigma Aldrich (Merck KGaA, Darmstadt, Germany). All the materials were analytical grade and were used.

2.2. Adsorption experiments

The batch adsorption studies were performed by mixing the solution containing phosphate ions and the adsorbent, using a magnetic stirrer. The size of the adsorbent material granules was between 0.063 and 2 mm. The retention of phosphate ions from the solution was calculated as the difference between the initial concentration and the concentration at different contact times. The amount removed per unit mass of adsorbent (a_t , mg/kg) at time "t" results from:

$$a_t = (C_0 - C_t) \frac{V}{m} \quad (1)$$

The removed percentage of phosphate ions was calculated from:

$$RP = \frac{C_0 - C_t}{C_0} 100 \quad (2)$$

Where a_t , mg/kg is the amount of phosphate ions removed per unit mass of the adsorbent at a given time, t ; C_0 , mg/L is the initial concentration of phosphate ions in the aqueous solution, C_t , mg/L is the concentration of phosphate ions at time, t ; V , L is the volume of the solution.

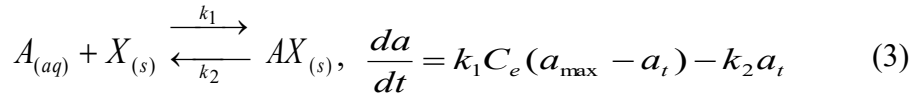
2.2.1. Kinetic study

The kinetic experimental determinations were made on PS at two pH values 3 and 9 and at a mass ratio of solid:liquid phases of 1:10. The pH was corrected with NaOH and H_2SO_4 solutions of 2M concentration. The samples were kept in contact with KH_2PO_4 solutions of variable concentrations 10, 20, 40, 60, 80 and 100 mg/L, for variable times 2, 5, 10, 15, 20, 30, 40, 60 minutes under stirring at 200 rpm, and the suspension was vacuum filtered. The resulting aqueous extract was analyzed according to SR ISO 6878:2005, Water quality — Determination of phosphorus — Ammonium molybdate spectrometric method.

First order Langmuir-Hinshelwood model adsorption model was used to fit the experimental data.

2.2.2. First order Langmuir-Hinshelwood model

To study phosphorous phosphate sorption rate in static conditions, it was used a Langmuir first order kinetic model which considers the chemosorption process, according to the following equation type [54]:



Where C_e is phosphate concentration in aqueous phase at equilibrium, mg/L; a_{\max} is maximum capacity of phosphate adsorption in PS, mg/kg; a_t is phosphate content in the PS at time t , mg/kg; k_1 is adsorption process rate constant, L/(mg·min); k_2 is desorption process rate constant, min⁻¹.

By changing the variables, equation (3) is linearized in the form:

$$y = AX_1 + BX_2 + C' \quad (4)$$

Where $A = k_1 \cdot a_{\max}$; $B = -k_2$; $C' = -k_1 C_e$; $X_1 = \frac{C_e}{a_t}$, $X_2 = C_e$ and

$$y = \frac{v}{a_t}.$$

3. Results and discussion

3.1. Kinetic study

From the mathematical processing of the experimental data based on the chemisorption model, the rate constants that describe the rapid and reversible sorption of phosphate ions retention in mobile forms on the surface of the adsorbent material (PS), were calculated. The variation of the amount of adsorbed phosphate depending on the contact time was achieved under the given conditions: the working pH was 3 and 9, the initial concentration of phosphate varied between 10-100 mg/L, at a mixing speed of 200 rpm. The adsorption of phosphate ions from aqueous solutions on PS was considerably influenced by the pH values. As pH values increased from 3 to 9, the average phosphate ions removed decreased.

The kinetic parameters calculated by linear regression according to the Langmuir-Hinshelwood first order mathematical model are presented in Table 4.

Table 4
Parameters of the kinetic model

pH	k_1 (mg ⁻¹ ·L ⁻¹ ·min ⁻¹)	k_2 (min ⁻¹)	K	a_{\max} (mg/kg)	R^2
3	$5.77 \cdot 10^{-4}$	$4.28 \cdot 10^{-2}$	$1,348 \cdot 10^{-2}$	2205.46	0.9021
9	$5.79 \cdot 10^{-4}$	$3.81 \cdot 10^{-2}$	$1.52 \cdot 10^{-2}$	1395.19	0.9049

Where $K = k_1/k_2$.

From the analysis of the kinetic parameters, it can be seen that adsorption increases with decreasing pH, the maximum loading can be observed at pH = 3, for all the concentration range. With the identified kinetic parameters graphical representation of experimental and calculated data are shown in Figs. 3 to Fig. 6.

The graphs that represent the data obtained according to the kinetic model are decreasing curves, with a sharper decrease at the beginning of the process (about 10 minutes), then they flatten out, as a result of the lower intensity of the sorption process.

From the point of view of pumice loading with phosphate ions, at pH = 3 the loading increases the most in the first 20 minutes, maximum 30 minutes, then the increase of pumice loading with phosphate ions after this time becomes much slower (Fig. 5 and Fig. 6). The graph showing the amount of phosphate removed at different time intervals on the pumice stone indicates that the initial phosphate removal increases with time but reaches a pseudo-equilibrium in time after 40 minutes. The process initially proved to be very fast and a large part of the total amount of phosphate is removed within a few minutes for the two values of the working pH. This may suggest that phosphate adsorption on pumice occurs through interactions between the adsorbent surface and phosphate ions with formation of Al and Ca phosphate salts.

At pH = 3 and at low initial concentrations of 10-20 mg/L, decreases to half of the initial concentration after a time of sixty minutes, and at higher concentrations decreases even more, to a third of the initial concentration. The most pronounced decrease is at pH = 3, and at pH = 9 the concentration decreases approximately by half (Fig. 3 and Fig. 4).

The maximum adsorption occurred at pH = 3, this being the optimal pH. In addition, the data in Fig. 3 show that the removal efficiency increases with contact time until it reaches equilibrium at about 60 minutes, then remains constant.

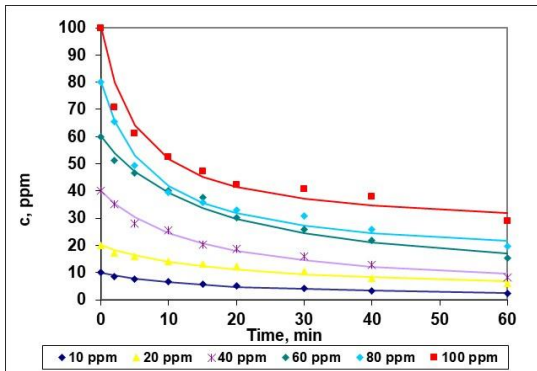


Fig. 3. Variation of phosphorus speciations concentration over time in the concentration range 10÷100 ppm at pH=3 (adsorption on PS)

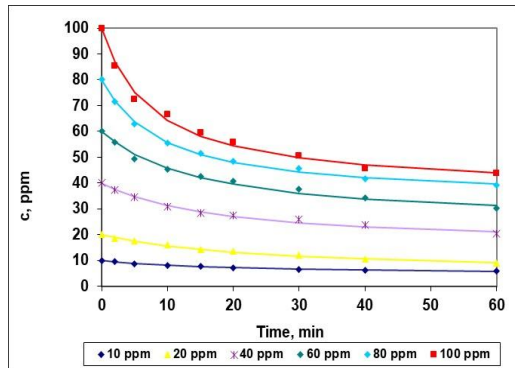


Fig. 4. Variation of phosphorus speciations concentration over time in the concentration range 10÷100 ppm at pH=9 (adsorption on PS)

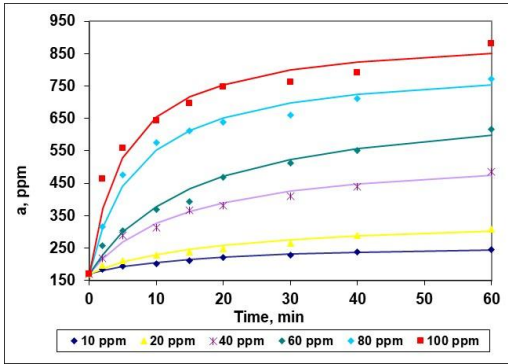


Fig. 5. Variation of loading over time in the concentration range 10÷100 ppm phosphate in the initial solution at pH = 3 (adsorption on PS).

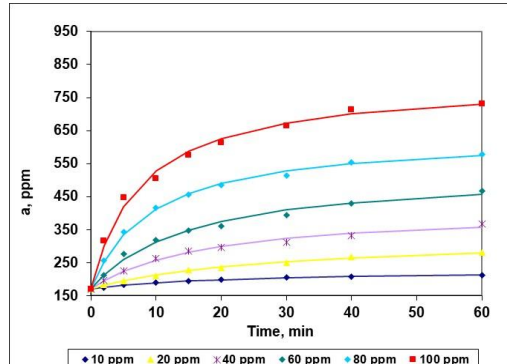


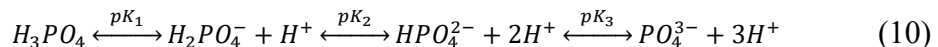
Fig. 6. Variation of loading over time in the concentration range 10÷100 ppm phosphate in the initial solution at pH = 9 (adsorption on PS)

Note: The points represent experimental data, and the line represents the calculated data according to the mentioned model

As it can be seen from Fig. 3, the highest phosphate ions removal rate was obtained at pH= 3. This can be explained by the fact that the pH of the solution influences both the surface charge of the PS and the nature of the phosphate ion (the degree and form in which the phosphate ion is dissociated). The effect of pH for the adsorption of the phosphate ion on the adsorbent surface can be associated with the relationship between pH and the electrical charge of the adsorbent surface.

Phosphate ions dissociation at different pH values [55].

Phosphate ions dissociate with pH in the following order:



The explanation can be attributed to the pH dependent solubility of iron and manganese oxides: at a pH lower than 6 iron and manganese oxides adsorb the phosphate ion from the solution. At pH lower than 8, adsorption takes place by ion exchange mechanism through the hydrolysis products of phosphate ions ($H_2PO_4^-$ și HPO_4^{2-}).

From the study of the speed variation over time (Figs. 7 and 8) it is found that the adsorption process proceeds at a very high speed in the first five minutes, but after 40 minutes the speed becomes almost zero, as a result of the saturation of the exchange positions. The adsorption rate decreases over time. The speed increases with increasing initial concentration of phosphate ions but has a similar behavior after 40 minutes regardless of the initial concentration value.

Adsorption takes place not only through interactions between the adsorbent and phosphate ions, but also through weak physical interactions between Al and Fe oxides and the surface of the adsorbent. The loading increases with time and decreases with increasing pH [21]. In a previously published study, it has been shown

that phosphate containing compounds adsorbed on materials that contain both CaO and Al_2O_3 promote the retention of phosphate by formation of AlPO_4 [21].

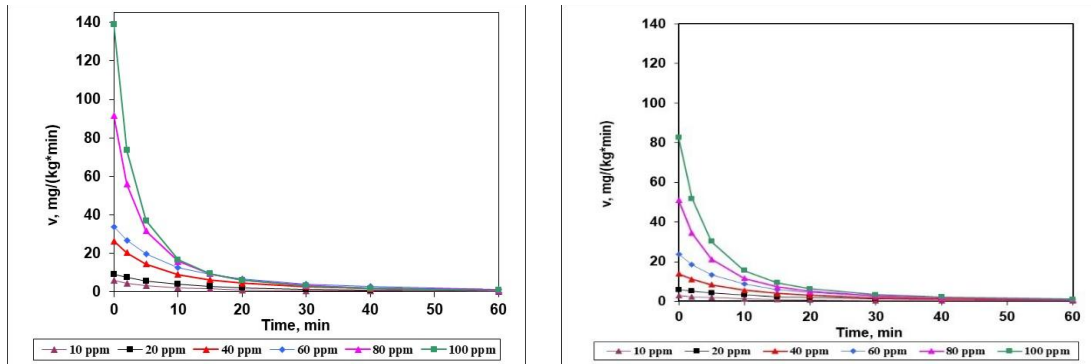


Fig. 7. Speed variation in the concentration range 10–100 ppm at pH = 3 (adsorption on PS)

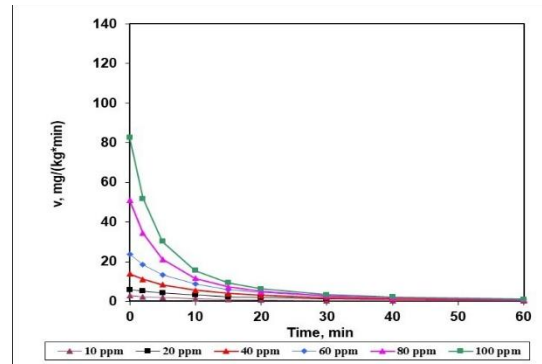


Fig. 8. Speed variation in the concentration range 10–100 ppm at pH = 9 (adsorption on PS)

Figs. 9 and 10 show the kinetic curves of constant speed at different concentrations and loadings of the PS. Through the graphical representation of the data obtained according to the model in the form of kinetic maps, two zones can be distinguished: an adsorption zone corresponding to constant velocity curves with positive values and a desorption zone corresponding to constant velocity curves with negative values. The zero-order kinetic curve delimits adsorption and desorption areas.

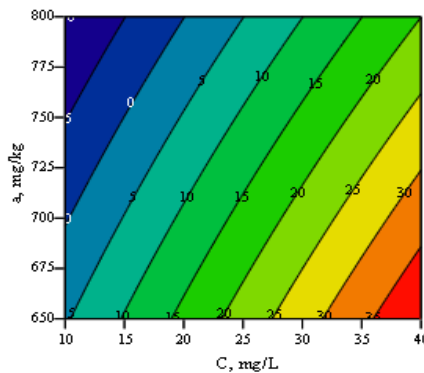


Fig. 9. Kinetic map of phosphate sorption on PS at pH = 3

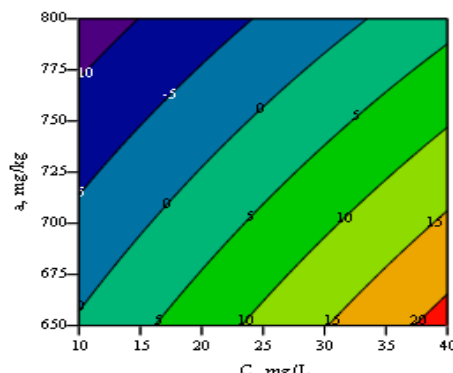


Fig. 10. Kinetic map of phosphate sorption on PS at pH = 9

Analyzing the kinetic map of the sorption of phosphate ions on PS at pH = 3, it can be observed that: adsorption processes are predominant, desorption processes take place with a very low intensity. At a constant loading of the PS with phosphate, as the concentration increases, the speed of the process also increases. From the analysis of the kinetic map of phosphate ions sorption on PS at pH = 9, it

can be observed that the desorption process intensifies more compared to pH = 3 and the adsorption processes decrease in intensity.

On the studied range of concentrations, both PS and ACC show higher adsorption capacity towards phosphate ions adsorption than previously reported studies [56]. Based on the quantities retained, phosphate adsorbed on either PS or ACC could be used in agriculture as a fertilizer [57-59].

Phosphate speciation depends on pH and affects its adsorption behavior. Maximum adsorption occurs at pH = 3, where H_2PO_4^- is the dominant species. In the pH range 2–8, phosphate adsorption is enhanced due to the positively charged adsorbent surface, whereas at pH > 8, excessive OH^- ions compete with phosphate, reducing its adsorption efficiency [60].

4. Conclusions

Water is an important resource that becomes even more valuable in the actual context of climate change. Concentrations of phosphorus phosphate ions in water, higher than what the living organisms existing in the ecosystem can consume, lead to the process of water eutrophication. This means that water quality is severely affected and leads to significant increase of water treatment cost.

Wastewater (resulted from urban, industrial, and agricultural activities) is the main source of phosphorous compounds. If it is directly discharged in the ecosystem will decrease the water quality.

Two adsorbent materials have been tested for phosphate removal from wastewater: pumice stone and autoclaved cellular concrete.

Characterization techniques of the two materials showed that they have good specific surface and a crystalline structure.

Initial phosphate ions adsorption increases with time, but a pseudo-equilibrium is reached in 40 minutes; the process initially proved to be very fast for the two pH values that have been tested. This may suggest that adsorption takes place via physical interactions initially; it is established that phosphate sorption on pumice stone, over time, is a slow process, illustrated by the values of the relatively small rate constants of these processes. It was found that the amount of phosphate adsorbed depends on the pH of the solution, a lower pH increasing the adsorbed amount for both tested materials. In this respect, the removal efficiency increases from 9 % at a pH of 9 to 90 % at a pH of 3. These results were attributed to the fact that the pH of the solution influences both the electrical charge of ACC and PS, and the type of phosphate ions.

Based on calculated parameters phosphate adsorption is favorable on both PS and ACC.

Adsorption occurs not only through interactions between the adsorbent and phosphate ions, but also through physical interactions between AlPO_4 and the surface of the adsorbent. The results of this study show that ACC and PS are

effective adsorbents for the removal of phosphate ions from aqueous solutions. The materials containing the phosphate ions could be used in fertilizers.

Limitations and perspectives

- Further testing on real wastewater containing mixtures of pollutants is still needed to assess the performance of the materials under real operating conditions. This study showed that PS (pumice stone) and ACC (autoclaved cellular concrete) are effective in removing phosphate ions from synthetic wastewater, especially in acidic pH conditions. However, to fully validate these materials for real-world applications, tests must be conducted on complex wastewater containing multiple contaminants. Adsorption might be inhibited by competing ions in real wastewater (e.g., PO_4^{3-} , SO_4^{2-} , HCO_3^-), although the presence of such competing ions was taken into account during the preparation of the synthetic wastewater. The simulated composition for phosphate-containing wastewater was as follows: PO_4^{3-} (10-100 mg/L), NO_3^- -N (20 mg/L), NH_4^+ (30 mg/L), SO_4^{2-} (100 mg/L), Cl^- (80 mg/L), HCO_3^- (120 mg/L), Na^+ (100 mg/L), Ca^{2+} (75 mg/L), Mg^{2+} (30 mg/L), K^+ (20 mg/L), COD (250 mg/L), pH 7.2, conductivity (1,500 $\mu\text{S}/\text{cm}$).
- In practice, the pH of wastewater is often in the neutral to alkaline range (7–9), where adsorption efficiency is lower compared to acidic conditions. This limitation can be overcome either by a simple pretreatment step to adjust the pH of the effluent or by enhancing the adsorbent materials through functionalization with metal oxides or hydroxides (e.g., aluminum, iron). These approaches can broaden the applicability of the materials under a wider range of operational conditions. At the same time, they align with current trends in the development of advanced phosphate removal technologies and provide a valuable foundation for future research.
- Although this study did not include experiments specifically focused on adsorption-desorption cycles, existing research suggests that materials like PS (pumice stone) and ACC (autoclaved cellular concrete) can be regenerated through alkaline or acidic washing, with minimal loss of capacity during the first few cycles [27, 28]. Therefore, a key direction for future research is to investigate the long-term durability of these materials over multiple cycles, as well as to determine the optimal regeneration conditions. The focus should be on maintaining adsorption capacity and preventing the release of metals into the solution. This step is crucial for assessing the feasibility of using these materials in continuous treatment scenarios, with an emphasis on both economic and environmental sustainability [46, 47].
- The low cost of PS (pumice stone) and ACC (autoclaved cellular concrete) gives them an advantage over methods like membrane separation or chemical precipitation. Besides adsorption using materials like PS and ACC, there are

other well-established methods for phosphate removal from wastewater, each with its own specific advantages and limitations. Chemical precipitation, which involves the use of iron, aluminum, or calcium salts, is effective and relatively affordable, but it generates large volumes of residual sludge. Membrane separation (such as ultrafiltration or reverse osmosis) offers high efficiency and the ability to remove other contaminants simultaneously, but it comes with significant costs related to energy use, fouling, and maintenance. Another increasingly studied alternative is crystallization (e.g., forming magnesium ammonium phosphate, or struvite), where magnesium, ammonium, and phosphate ions form a solid precipitate that can be used as fertilizer [12-14, 19-21]. This method enables resource recovery, but it requires precise pH control (between 8–9) and an optimal molar ratio of Mg:N:P, which can make it more expensive compared to simple adsorption. In this context, porous materials like PS and ACC stand out for their low operational costs (€0.05–0.15/m³), technological simplicity, and potential for integration into hybrid systems [58]. They can also serve as decentralized or complementary solutions depending on the type of effluent and the treatment goals.

Pumice stone and autoclaved aerated concrete are promising sorbents for the efficient removal of phosphates, contributing both to the treatment of acidic waters—such as those polluted by mining or chemical industries—and basic waters, such as those resulting from certain industrial processes or improperly treated effluents, while also enabling phosphate ions recovery. So make them excellent candidates for integration into current wastewater treatment schemes—either as standalone systems for decentralized treatment or as components in hybrid processes.

R E F E R E N C E S

- [1] Y. Ding; Q. Yi, Q. Jia, Zhang, J.; Z. Zhou, X. Liu, Quantifying phosphorus levels in water columns equilibrated with sediment particles in shallow lakes: From algae/cyanobacteria-available phosphorus pools to pH response. *Sci. Total Environ.*, **666**, pp. 39-45, 2023
- [2] X. Bai, J. Sun, Y. Zhou, L. H Gu Zhao, J. Wang, Variations of different dissolved and particulate phosphorus classes during an algae bloom in a eutrophic lake by ³¹P NMR spectroscopy. *Chemosphere*, **169**, pp. 577-585, 2017
- [3] G. Simoni, P. Cheali; P. Roslev, Haasler, K. Reitzel, A. M. Smith; M. H. Sahl Haferbier Lykkegaard Christensen, M. Flocculating and dewatering of lake sediment: An in-situ pilot study comparing synthetic polymers and biopolymers for restoring lake water quality and reusing phosphorus. *Sci. Total Environ.*, **913**, pp. 169597, 2024
- [4] B. Garske, J. Stubenrauch, F. Ekardt, Sustainable phosphorus management in European agricultural and environmental law. *RECIEL*, **29(1)**, pp. 107-117, 2020
- [5] Council Directive 91/271/EEC of 21 May 1991 concerning urban waste-water treatment, <https://eur-lex.europa.eu/eli/dir/1991/271/oj> (Accessed on 11th of February 2024).
- [6] Consolidated text: Council Directive of 21 May 1991 concerning urban wastewater treatment (91/271/EEC), <https://eur-lex.europa.eu/legal-content/EN/TXT/?uri=CELEX%3A01991L0271-20140101> (Accessed on 11th of February 2024).
- [7] X. Chen, Y. Wang, Z. Bai, L. Ma, M. Strokal, C. Kroese, X. Chen,; Zhang, F.; Shi, X. Mitigating phosphorus pollution from detergents in the surface waters of China. *Sci. Total Environ.*, **804**, pp. 150125, 2022

[8] *J. Liu, W. Gu, Y. Liu, C. Zhang, W. Li, Shao, D.* Dynamic characteristics of net anthropogenic phosphorus input and legacy phosphorus reserves under high human activity - A case study in the [9] Jianghan Plain. *Sci. Total Environ.*, 836, pp. 155287, 2022

[10] *M. Cui, Q. Guo, R. Wei, L. Tian* Human-driven spatiotemporal distribution of phosphorus flux in the environment of a mega river basin. *Sci. Total Environ.*, 752, pp. 141781, 2021.

[11] *L. Hoang, L.; Mukundan, R.; Moore, K. E.B.; Owens, E. M.; Steenhuis, T. S.* Phosphorus reduction in the New York City water supply system: A water-quality success story confirmed with data and modelling. *Ecol. Eng.*, 135, pp. 75-88, 2019

[12] *L. Deng, B. R. Dhar*, Phosphorus recovery from wastewater via calcium phosphate precipitation: A critical review of methods, progress, and insights. *Chemosphere*, 330, pp. 138685, 2023.

[13] *Md. M. Rahman, M. A. Mohd. Salleh, U. Rashid, A. Ahsan, M. M. Hossain, C. S. Ra*, Production of slow release crystal fertilizer from wastewaters through struvite crystallization – A review. *Arab. J. Chem.*, 7, pp. 139-155, 2014

[14] *A. Mayhunru, S. Foteinis, R. Mbaya, V. Masindi, I. Kortidis, L. Mpenyana-Monyatsi, E. Chatzisymeon* Environmental sustainability of municipal wastewater treatment through struvite precipitation: Influence of operational parameters. *J. Clean. Prod.*, 285, pp. 124856, 2021

[15] *W. Almanassra, G. Mckay, V. Kochkodan, M.A. Atieh, T. Al-Ansari* A state of the art review on phosphate removal from water by biochars. *Chem. Eng. J.*, 409, pp. 128211, 2021

[16] *Z. Zhan, R. Wang, M. Saakes, R.D. Van der Weijden, C.J.N. Buisman, Y. Lei* Basket anode filled with CaCO_3 particles: A membrane-free electrochemical system for boosting phosphate recovery and product purity. *Water Res.*, 231, pp. 119604, 2023

[17] *X. Li, S. Shen, Y. Xu, T. Guo, H. Dai, X. Lu* Application of membrane separation processes in phosphorus recovery: A review. *Sci. Total Environ.*, 767, pp. 144346, 2021

[18] *G. Qiu, S. Zhang, D.S.S. Raghavan, S. Das, Y.-P. Ting* The potential of hybrid forward osmosis membrane bioreactor (FOMBR) processes in achieving high throughput treatment of municipal wastewater with enhanced phosphorus recovery. *Water Res.*, 105, pp. 370-382, 2016

[19] *Q. Zhou, H. Sun, L.W. Jia, J. Wu, Wang*. Simultaneous biological removal of nitrogen and phosphorus from secondary effluent of wastewater treatment plants by advanced treatment: A review. *Chemosphere*, 296, pp. 134054, 2022

[20] *X. Jin, J. Guo, Md. F. Hossain, J. Lu, Q. Lu, Y. Zhou, Y. Zhou*, Recent advances in the removal and recovery of phosphorus from aqueous solution by metal-based adsorbents: A review. *Resour. Conserv. Recycl.*, 204, pp. 107464, 2024

[21] *X. Fan, Y. Wu, Y. He, H. Liu, J. Guo, B. Li Peng, H.* Efficient removal of phosphorus by adsorption. *Phosphorus Sulfur Silicon Relat. Elem.*, 198, pp. 375-384, 2023

[22] *E. Oguz, A. Gurses, M. Yalcin* Removal of phosphate from waste waters by adsorption. *Water, Air Soil Pollut.*, 148, pp. 279-287, 2003

[23] *N. Che, J. Qu, J. Wang, N. Liu, C. Li, Y. Liu* Adsorption of phosphate onto agricultural waste biochars with ferrite/manganese modified-ball-milled treatment and its reuse in saline soil. *Sci. Total Environ.*, 915, pp. 16984, 2024

[24] *J.H. Sterba, K.P. Foster, G. Steinhauser, M. Bichler* New light on old pumice: the origins of Mediterranean volcanic material from ancient Egypt. *J. Archaeol. Sci.*, 36, pp. 1738-1744, 2009

[25] *W. Pungarasi, P. Phinitthanaphak, S. Powtongsook* Nitrogen removal from a recirculating aquaculture system using a pumice bottom substrate nitrification-denitrification tank. *Ecol. Eng.*, 95, pp. 357-363, 2016

[26] *T. Liu, Z-L. Wang, X. Yan, B. Zhang* Removal of mercury (II) and chromium (VI) from wastewater using a new and effective composite: Pumice-supported nanoscale zero-valent iron. *Chem. Eng. J.*, 245, pp. 34-40, 2014

[27] *M.N. Sepehr, A. Amrane, K.A. Karimaian, M. Zarrabi, H.R. Ghaffari* Potential of waste pumice and surface modified pumice for hexavalent chromium removal: Characterization, equilibrium, thermodynamic and kinetic study. *J. Taiwan Inst. Chem. Eng.*, 45, pp. 635-647, 2014

[28] *H. Soleimani, A.H. Mahvi, K. Yaghmaeian, A. Abbasnia, K. Sharafi, M. Alimohammadi, M. Zamanzadeh* Effect of modification by five different acids on pumice stone as natural and low-cost adsorbent for removal of humic acid from aqueous solutions - Application of response surface methodology. *J. Mol. Liq.*, 290, pp. 111181, 2019

[29] *B. Heibati, S. Rodriguez-Couto, N.G. Turan, O. Ozgonenel, A.B. Albadarin, M. Asif, I. Tyagi, S. Agarwal, V.K. Gupta* Removal of noxious dye—Acid Orange 7 from aqueous solution using natural pumice and Fe-coated pumice stone. *J. Ind. Eng. Chem.*, 31, pp. 124-131, 2015

[30] *M. Subrahmanyam, P. Boule, V. Durga Kumari, D. Naveen Kumar, M. Sancelme, A. Rachel* Pumice stone supported titanium dioxide for removal of pathogen in drinking water and recalcitrant in wastewater. *Sol. Energy*, 82(12), pp. 1099-1106, 2008

[31] Multidimensional classification of magma types for altered igneous rocks and application to their tectonomagmatic discrimination and igneous provenance of siliciclastic sediments. *Lithos*, 278–281, pp. 321-330, 2017

[32] *M.A. Gatea, G.F. Jumaah, R.H. Al anbari, Q.F. Alsalhy* Decontaminating liquid-containing Cs-137 by natural Pumice stone. *J. Environ. Radioact.*, 272, pp. 107342, 2024

[33] *Z. Pavlik, M. Vysvaril, S.P. Verma, M. Ab. Rivera-Gómez, L. Díaz-González, K. Pandarinath, A. Amezcu-Valdez, M. Rosales-Rivera, S.K. Verma, A. Quiroz-Ruiz, J.S. Armstrong-Altrin M. Pavlikova, P. Bayer, A. Pivak, P. Rovnanikova, M. Zaleska* Lightweight pumice mortars for repair of historic buildings – Assessment of physical parameters, engineering properties and durability, *Constr. Build. Mater.*, 404, pp. 133275, 2023

[34] *I.H. Nurwahid, L.C.C. Dimonti, A.A. Dwiatmoko, J.-M. Ha, R.T. Yunarti*, Investigation on SiO₂ derived from sugarcane bagasse ash and pumice stone as a catalyst support for silver metal in the 4-nitrophenol reduction reaction. *Inorg. Chem. Commun.*, 135, pp. 109098, 2022

[35] *S. Senorans, J.R. Díaz, D. Escalante, L.A. Gonzalez, L. Díaz* Ce/Pumice and Ni/Pumice as heterogeneous catalysts for syngas production from biomass gasification. *Waste Manag.*, 166, pp. 270-279, 2023

[36] *P.Y. Motlagh, S. Akay, B. Kayan, A. Khataee* Ultrasonic assisted photocatalytic process for degradation of ciprofloxacin using TiO₂-Pd nanocomposite immobilized on pumice stone. *J. Ind. Eng. Chem.*, 104, pp. 582-591, 2022

[37] *Y.H. Gad, R.H. Helal, H. Radi, K.F. El-Nemr, E.E. Khozemy*, Preparation and application of irradiated polyvinyl alcohol/starch/pumice composites for adsorption of basic dye: Isotherm and kinetics study. *Int. J. Biol. Macromol.*, 249, pp. 126106, 2023

[38] *Y. Zhang, G.-S. Xu, M.-D. Xu, D.-C. Wang, H. Wang, Y. Zhan, Z. Jin* Preparation of MgO porous nanoplates modified pumice and its adsorption performance on fluoride removal. *J. Alloys Compd.*, 884, pp. 160953, 2021

[39] *M. Kasraee, M.H. Dehghani, A.H. Mahvi, R. Nabizadeh, M.M. Arjmand, M. Salari, F. Hamidi, N.M. Mubarak, I. Tyagi* Adsorptive removal of humic substances using cationic surfactant-modified nano pumice from water environment: Optimization, isotherm, kinetic and thermodynamic studies, *Chemosphere*, 307, pp. 135983, 2022

[40] *G. Asgari, B. Roshani, G. Ghanizadeh* The investigation of kinetic and isotherm of fluoride adsorption onto functionalized pumice stone. *J. Hazard. Mater.*, 217–218, pp. 123-132, 2012

[41] *R.A. Iernutan, F. Babota* Autoclaved Cellular Concrete (ACC) Masonry with Vertical Hollows Confined with Disperse Reinforced Concrete. *Procedia Eng.*, 181, pp. 300-307, 2017

[42] *S.S. Mousavi, M. Dehestani* Influence of mixture composition on the structural behaviour of reinforced concrete beam-column joints: A review. *Structures*, 42, pp. 29-52, 2022

[43] *M.S. Goual, A. Bali, F. De Barquin, R.M. Dheilly, M. Quénéudec*, Isothermal moisture properties of Clayey Cellular Concretes elaborated from clayey waste, cement and aluminium powder. *Cem. Concr. Res.*, 36, pp. 1768–1776, 2006

[44] *M. Lei, S. Deng, K. Huang, Z. Liu, F. Wang, S. Hu*, Preparation and characterization of a CO₂ activated aerated concrete with magnesium slag as carbonatable binder. *Constr. Build. Mater.*, 353, pp. 129112, 2022

[45] *J. Suave, S.M. Amorim, R.F.P.M Moreira* TiO₂-graphene nanocomposite supported on floating autoclaved cellular concrete for photocatalytic removal of organic compounds. *J. Environ. Chem. Eng.*, 5(4), pp. 3215-3223, 2017

[46] *D. Martemianov, B.-B. Xie, T. Yurmanova, M. Khaskelberg, F. Wang, C.-H. Wei, S. Preis* Cellular concrete-supported cost-effective adsorbents for aqueous arsenic and heavy metals abatement. *J. Environ. Chem. Eng.*, 5(4), pp. 3930-3941, 2017

[47] *F.V. De Andrade, G.M. De Lima, R. Augusti, M.G. Coelho, J.D. Ardisson, O.B.A. Romero* versatile approach to treat aqueous residues of textile industry: The photocatalytic degradation of Indigo Carmine dye employing the autoclaved cellular concrete/Fe₂O₃ system. *J. Chem. Eng.*, 180, pp. 25–31, 2012

[48] *F.V. De Andrade, G.M. De Lima, R. Augusti, J.C.C. Da Silva, M.G. Coelho, R. Paniago, I.R. Machado* A novel TiO₂/autoclaved cellular concrete composite: From a precast building material to a new floating photocatalyst for degradation of organic water contaminants *J. Water Proc. Engineering*, 7, pp. 27–35, 2015

- [49] *M. Du, Y. Zhang, Z. Wang, M. Lv, A. Tang, Y. Yu, X. Qu, Z. Chen, Q. Wen, A. Li* Insight into the synthesis and adsorption mechanism of adsorbents for efficient phosphate removal: Exploration from synthesis to modification. *Chem. Eng J.*, 442, pp. 136147, 2022
- [50] *G.A. Saygılı, F. Güzel* Chemical modification of a cellulose-based material to improve its adsorption capacity for anionic dyes. *J. Dispers. Sci. Technol.*, 38(3), pp. 381–392, 2017
- [51] *Z. Elkhlifi, A.H. Lahori, I.I. Shahib, J. Iftikhar, S. Wang* Comparative assessment of phosphate adsorption properties and mechanisms on Mg/Al-engineered sewage sludge biochar in aqueous solution. *J. Water Proc.Engineering*, 56, pp. 104443, 2023
- [52] *S. Karaca, A. Gürses, M. Ejder, M. Açıkyıldız* Kinetic modeling of liquid-phase adsorption of phosphate on dolomite. *J. Colloid Interface Sci.*, 277, pp. 257–263, 2004
- [53] *A. Yu Kudeyarova* Chemisorption of phosphate ions and destruction of organomineral sorbents in acid soils. *Soil Chem.*, 2010, 43, pp. 635–650.
- [54] *J.G. Prato, F.C. Millán, L.C. González, A.C. Ríos, E. López, I. Ríos, S. Navas, A. Márquez, J. C. Carrero, J.I. Díaz* Adsorption of Phosphate and Nitrate Ions on Oxidic Substrates Prepared with a Variable-Charge Lithological Material. *Water*, 14(16), pp. 2454, 2022
- [55] *W. Rudzinski, T. Panczyk*, The Langmuirian Adsorption Kinetics Revised: A Farewell to the XXth Century Theories? *Adsorption*, 8, pp. 23–34, 2002
- [56] *A. Zhou, H. Tang, D. Wang* Phosphorus adsorption on natural sediments: Modeling and effects of pH and sediment composition. *Water Res.*, 39, pp. 1245–1254, 2005
- [57] *V. Patyal, D. Jaspal, K. Khare* Materials for phosphorous remediation: a review, *Phosphorus Sulfur Silicon Relat. Elem.*, 196(12), pp. 1025–1037, 2021
- [58] *Kataki, S.; West, H.; Clarke, M.; Baruah, D.C.* Phosphorus recovery as struvite: Recent concerns for use of seed, alternative Mg source, nitrogen conservation and fertilizer potential. *Resour. Conserv. Recycl.*, 107, pp. 142–156, 2016
- [59] *L. Pérez-Urrestarazu, R. Fernández-Cañero, P. Campos-Navarr, C. Sousa-Ortega, G. Egea* Assessment of perlite, expanded clay and pumice as substrates for living walls. *Sci. Hortic.*, 254, pp. 48-54, 2019
- [60] *Aimin Zhou, Hongxiao Tang, Dongsheng Wang*, Phosphorus adsorption on natural sediments: Modeling and effects of pH and sediment composition, *Water Research* 39, pag. 1245–1254, 2005